An *ab initio* study of solvent shifts in vibrational spectra

Eugene V. Stefanovich[a] and Thanh N. Truong[b]
Department of Chemistry, University of Utah, Salt Lake City, Utah 84112

(Received 26 March 1996; accepted 15 May 1996)

Using analytical second derivatives of the generalized conductorlike screening model (GCOSMO) we calculate vibrational frequency shifts for several molecules (acetone, methylamine, formic acid, acetic acid, and trans-NMA) solvated in water. In these calculations, results from dielectric continuum approach with and without several explicit water molecules are compared with traditional supermolecule approach. The simple GCOSMO model, where all solvent molecules are treated as a continuum medium, reproduces quite accurately solvent shifts in solutes having moderate hydrogen bondings with water, such as acetone and methylamine. To represent strong solvent effects in formic acid and acetic acid, one should add at least one explicit water molecule in GCOSMO calculations. Solvent effects on solute structure correlate well with frequency shifts. Geometry optimizations and frequency calculations in the GCOSMO-supermolecule approach require only 10%–20% more computational effort than similar calculations in the gas phase. Therefore, this method provides a promising and effective tool for studying reactivity, structural, and spectroscopic properties of realistic solutes. © *1996 American Institute of Physics.* [S0021-9606(96)02032-6]

I. INTRODUCTION

Vibrational frequencies provide important information about chemical bonding in solutions and solute–solvent interactions. Currently there are two major theoretical approaches for *ab initio* calculations of vibrational spectra in solutions. In the *supermolecule* approach, a solvated system is modeled by a molecular complex of the solute with a small number of solvent molecules in vacuo.[1] Although analytical first and second derivatives are available for efficient geometry optimization and frequency calculations,[2] the large size of the quantum mechanical system makes these calculations rather expensive and prohibits use of large basis sets and high levels of theory. These restrictions usually result in large 10%–20% errors in calculated vibrational frequencies. This problem was addressed by introducing the *scaled quantum mechanical force field* (SQMFF) methodology[3] within the supermolecule approach. In such calculations some of calculated force constants are scaled to reproduce experimental data for both gas phase and solvated species.[4–10] Although this scaling procedure allows one to obtain valuable information about the solvent effect on the molecular force field, the predictive power of such calculations is limited. In the supermolecule method, hydrogen bonds with neighboring water molecules are represented quite accurately; however, it is difficult to take into account the long-range polarization of the solvent due to the large number of explicit water molecules required. A related approach was employed in Refs. 11 and 12 for studying vibrational spectrum of hydrated glycine zwitterion where the intramolecular force field derived from *ab initio* calculation of isolated solute was coupled with classical molecular dynamics simulation of the solute interacting with several hundred water molecules.

In the *dielectric continuum approach* (for a recent review, see Ref. 13), the dielectric polarization effect is modelled by approximating the solvent as a uniform dielectric medium. An important progress was achieved in the Self-Consistent Reaction Field Method[14,15] based on the Onsager solvation model. Analytical first and second derivatives are available for this method, so that geometry optimization and frequency calculations can be performed quite effectively (see also Ref. 16). In this approach, the solvent is placed inside a spherical or ellipsoidal cavity in a homogeneous dielectric medium and the charge distribution of the solute is approximated by a multipolar expansion. The use of spherical and ellipsoidal cavities is not justified for most solutes. More general cavity shapes can be employed with the use of reaction field factors.[17] This approach allows for efficient calculations of first energy derivatives and geometry optimization;[18] however, no applications of second derivatives were reported thus far. An accurate self-consistent description of the solute charge density in realistic molecular-shape cavities is provided by the Polarizable Continuum Model (PCM) developed by Tomasi *et al.*[19] However, the character of the PCM equations results in a quite complicated form for the analytical first and second energy derivatives.[20,21] This makes it rather difficult to optimize the geometry of the solvent and calculate vibrational frequencies. Up to now, vibrational spectra of only small model solutes, like HF and H_2O, have been studied by the PCM method using numerical second derivatives.[22–24]

Recently, we proposed the *ab initio* generalized conductorlike screening model (GCOSMO)[25–28] which is a generalization of the semiempirical COSMO model suggested by Klamt and Schüürmann.[29] Similar to the PCM model, GCOSMO uses exact solute potential derived from *ab initio* self-consistent calculation of the solute inside a molecular-

[a]On leave from: The Institute of Chemical Physics, University of Latvia, 19 Rainis Blvd., Riga, LV 1586, Latvia.
[b]Author to whom correspondence should be addressed.

shape cavity. The boundary conditions of the GCOSMO model provide a good approximation to the exact Poisson boundary conditions of the PCM model; however, as described earlier, the GCOSMO approach offers significant computational advantages as compared to the PCM. Most importantly, first and second energy derivatives can be calculated in a simple and effective manner.[26] This opens new possibilities for routine geometry optimization and frequency calculations for rather complex solutes.

The major drawback of all dielectric continuum models is the neglect of specific hydrogen bonds between the solute and solvent molecules. On the other hand, the supermolecule approach disregards the dielectric polarization of the solvent. Both these effects play an important role in structure and vibrational spectra in solutions and should be taken into account self-consistently.[30–33] Furthermore, electron correlation effects should be properly represented if one is interested in quantitative prediction of vibrational spectra in both gas phase and solution.

The above considerations suggest the following main features for any realistic theoretical model designed to study vibrational spectra in solutions. First, a sufficient number of explicit water molecules should be included in calculation in order to represent strong specific solute–solvent hydrogen bonds. Second, dielectric polarization effects should be taken into account, for instance by placing the supermolecular complex inside a molecular-shaped dielectric cavity with an appropriate dielectric continuum boundary condition. Such a boundary condition must be suitable for efficient calculation of the first and second energy derivatives with respect to nuclear coordinates. Third, extended basis sets should be used and electron correlation effects should be taken into account for accurate representation of the solute charge density, force field, and interactions with both discrete and continuous solvent.

To meet these challenges, in this paper we use the GCOSMO dielectric continuum model in conjunction with discrete representation of several water molecules. In contrast to previous approaches relying on HF-based methods, we use here nonlocal density functional theory which has been proven accurate and efficient in studying ground state properties of molecules such as geometry and vibrational frequencies.[34,35] However, our main interest is not in absolute values of vibrational frequencies in solution—their accurate calculation requires rather sophisticated correlated levels of theory and sufficiently large basis sets. We are more interested in assessing the accuracy of the GCOSMO solvation model in the calculation of frequency shifts.

The main purpose of this paper is to assess the accuracy of the method outlined above and to demonstrate important effects of both specific hydrogen bonds and dielectric reaction field on hydration shifts of vibrational frequencies. To do this we have performed frequency shift calculations for acetone, methylamine, formic acid, acetic acid, and trans-N-methylacetamide (NMA). Several considerations determined this choice of solutes. First, comparison of our results with reliable experimental and theoretical data for both gas phase and hydrated molecules is possible. Second, these solutes have quite different strengths of hydrogen bonding with water ranging from moderate (acetone) to very strong (formic acid). This gives an opportunity to study both dielectric polarization and hydrogen bonding effects for qualitatively different solvent–solute interactions of various solute functional groups. Finally, trans-NMA is the simplest model of the peptide bond and therefore attracts much interest in both theoretical and experimental biological chemistry.

In Sec. II, we present basic equations for GCOSMO calculations of the free energy and its first derivatives in polar solvents.[25,26] We also derive expressions for the second energy derivatives which are useful for calculating vibrational frequencies. In Sec. III, results of frequency calculations are compared for different representations of the solvent: discrete, continuum, and discrete–continuum. These results are discussed in Sec. IV where we focus on solvent effects on structure and vibrational frequencies and relationships between these properties. Conclusions are summarized in Sec. V.

II. GENERALIZED CONDUCTORLIKE SCREENING MODEL (GCOSMO)

A. Energy and gradients

The essence of the GCOSMO method is first to determine the surface charges $\sigma(\mathbf{r})$ on the surface S of the molecular cavity in the case of a screening conductor (the dielectric constant $\varepsilon=\infty$) from a boundary condition that the total electrostatic potential on the surface S is zero,

$$\sum_i \frac{z_i}{|\mathbf{r}-\mathbf{R}_i|} - \int_V \frac{\rho(\mathbf{r}')}{|\mathbf{r}-\mathbf{r}'|}\, d^3r' + \int_S \frac{\sigma(\mathbf{r}')}{|\mathbf{r}-\mathbf{r}'|}\, d^2r' = 0, \tag{1}$$

where $\mathbf{r}$ is on S, ρ is the solute electron density, and z_i and $\mathbf{R}_i$ are the nuclear charge and position vector of solute atom i. For a dielectric medium specified by the dielectric constant ε, actual surface charges are then determined approximately by scaling the screening conductor surface charge $\sigma(\mathbf{r})$ by a factor of $f(\varepsilon)=(\varepsilon-1)/\varepsilon$ to satisfy the Gauss theorem for the total surface charge. For polar solvents, like water, this is a good approximation to the exact Poisson boundary condition.

In the boundary element method, the cavity boundary S is divided into M surface elements with areas $\{S_u\}$, and surface charge density at each surface element is approximated as a point charge, $\{q_u\}$, located at the center of that element, $\{\mathbf{t}_u\}$. In this approximation, the vector of surface charges is given by

$$\mathbf{q} = -f(\varepsilon)\mathbf{A}^{-1}(\mathbf{Bz}+\mathbf{c}), \tag{2}$$

where $\mathbf{z}$ is the vector of N nuclear charges and $\mathbf{A}$, $\mathbf{B}$, and $\mathbf{c}$ are $M\times M$, $M\times N$, and $M\times 1$ matrices, respectively, with matrix elements defined by[29]

$$A_{uv} = \frac{1}{|\mathbf{t}_u-\mathbf{t}_v|} \quad \text{for } u\neq v, \text{ and } A_{uu} = 1.07\sqrt{\frac{4\pi}{S_u}}, \tag{3}$$

$$B_{ui}=\frac{1}{|\mathbf{t}_u-\mathbf{R}_i|}, \tag{4}$$

$$c_u=-\int \frac{\rho(\mathbf{r})}{|\mathbf{r}-\mathbf{t}_u|}\, d^3r. \tag{5}$$

Alternatively, these surface charges can be determined by variationally minimizing the total electrostatic solvation energy

$$\Delta G_{\rm els}(\mathbf{q})=\mathbf{z}^\dagger\mathbf{B}^\dagger\mathbf{q}+\mathbf{c}^\dagger\mathbf{q}+\frac{1}{2\,f(\varepsilon)}\,\mathbf{q}^\dagger\mathbf{A}\mathbf{q} \tag{6}$$

with respect to $\mathbf{q}$ († denotes matrix transposition).

By expanding c_u given by Eq. (5) in a basis set, we obtain

$$c_u=\sum_{\mu\nu} P_{\mu\nu}L^u_{\mu\nu}, \tag{7}$$

where

$$L^u_{\mu\nu}=-\left\langle \mu\left|\frac{1}{\mathbf{r}-\mathbf{t}_u}\right|\nu\right\rangle \tag{8}$$

are one-electron integrals similar to those used for calculation of the electron–nuclear attraction, and $P_{\mu\nu}$ is the density matrix which includes solvent effects. The total free energy of the whole system (solute+surface charges) in the Hartree–Fock approximation is then given by

$$E_{\rm tot}=\sum_{\mu\nu}\,[P_{\mu\nu}(H^0_{\mu\nu}+H^s_{\mu\nu})+\tfrac{1}{2}\,P_{\mu\nu}(G^0_{\mu\nu}+G^s_{\mu\nu})] - \tfrac{1}{2}\,f(\varepsilon)\mathbf{z}^+\mathbf{B}^+\mathbf{A}^{-1}\mathbf{B}\mathbf{z}+E_{nn}+E_{\rm non\text{-}els}, \tag{9}$$

where E_{nn} is the solute nuclear repulsion and $E_{\rm non\text{-}els}$ is the nonelectrostatic part of the free energy of solvation that includes the dispersion, repulsion, and cavity formation contributions. Here $H^0_{\mu\nu}$ and $G^0_{\mu\nu}$ are, respectively, the one-electron and two-electron parts of the Fock matrix for isolated solute. The solvent contributions to these operators are expressed as

$$H^s_{\mu\nu}=-f(\varepsilon)\mathbf{z}^\dagger\mathbf{B}^\dagger\mathbf{A}^{-1}\mathbf{L}_{\mu\nu}, \tag{10}$$

$$G^s_{\mu\nu}=-f(\varepsilon)\left(\sum_{\lambda\sigma} P_{\lambda\sigma}\mathbf{L}^\dagger_{\lambda\sigma}\right)\mathbf{A}^{-1}\mathbf{L}_{\mu\nu}. \tag{11}$$

In the density functional approach, a similar expression for the free energy is valid if the exchange part of the operator $G^0_{\mu\nu}$ is replaced with the density-dependent exchange-correlation potential.[34]

The major contribution to derivatives of the free energy (9) for polar solutes comes from three first (electrostatic) terms on the right-hand side of Eq. (9).[26] For nonpolar and hydrophobic solutes, derivatives of the nonelectrostatic solvation energy may become important;[36] however, they are neglected in the present work. The electrostatic part of the free energy can be rewritten as

$$E=\sum_{\mu\nu}\,[P_{\mu\nu}H^0_{\mu\nu}+\tfrac{1}{2}\,P_{\mu\nu}G^0_{\mu\nu}]+E_{nn}+\Delta G_{\rm els}, \tag{12}$$

where $\Delta G_{\rm els}$ is given by Eq. (6).

Differentiating this equation with respect to a nuclear coordinate x and using the surface charges from Eq. (2), we obtain

$$\frac{\partial E}{\partial x}=\sum_{\mu\nu} P_{\mu\nu}\frac{\partial H^0_{\mu\nu}}{\partial x}+\frac{1}{2}\sum_{\substack{\mu\nu\\ \lambda\sigma}} P_{\mu\nu}P_{\lambda\sigma}\frac{\partial(\mu\lambda\|\nu\sigma)}{\partial x} -\sum_{\mu\nu} W_{\mu\nu}\frac{\partial S_{\mu\nu}}{\partial x}+\frac{\partial E_{nn}}{\partial x}+\mathbf{z}^\dagger\frac{\partial\mathbf{B}^\dagger}{\partial x}\,\mathbf{q} +\sum_{\lambda\sigma} P_{\lambda\sigma}\frac{\partial\mathbf{L}^\dagger_{\lambda\sigma}}{\partial x}\,\mathbf{q}+\frac{1}{2\,f}\,\mathbf{q}^\dagger\frac{\partial\mathbf{A}}{\partial x}\,\mathbf{q}, \tag{13}$$

where $W_{\mu\nu}$ is an energy-weighted density matrix containing solvent effects. The four first terms in Eq. (13) are the same as for the HF or Kohn–Sham theory for a molecule in vacuo.[2,35] The last three terms in Eq. (13) are due to the electrostatic solvation energy. Derivatives of matrices $\mathbf{A}$ and $\mathbf{B}$ were calculated in Ref. 26, and $\partial\mathbf{L}^\dagger_{\lambda\sigma}/\partial x$ are similar to derivatives of nuclear attraction integrals.

B. Analytical second derivatives

To obtain analytical second derivatives of the GCOSMO model for frequency calculations, it is not appropriate to differentiate formally the expression for first derivatives in Eq. (13). Such differentiation is valid only in the case of pure equilibrium solvation; however, the solvent response on solute vibrations has contributions from both equilibrium and nonequilibrium solvation effects.[13] The solvent dielectric response on solute vibrations can be approximately divided into two components: electronic (fast) and orientational (slow).[37] The fast component is mainly due to the electronic polarizability of water molecules. Macroscopically, this part of polarization is described by the high-frequency dielectric constant ε_∞, and corresponding polarization field instantly adjusts itself to the charge distribution of the solute. In the GCOSMO approach this part of polarization is described by the ''electronic'' surface charge density $\sigma_{el}=[(\varepsilon_\infty-1)/\varepsilon_0]\sigma$ (see, for instance, Ref. 38), where σ is the screening conductor charge density. The slow polarization component corresponds to reorientational movements of water molecules with low characteristic frequencies. For high-frequency solute vibrations, this part of the surface charge density $\sigma_{or}=[(\varepsilon_0-1)/\varepsilon_0]\sigma-\sigma_{\rm el}$ can be assumed fixed. Moreover, the shape of the cavity, which is determined by the positions of water molecules around the solute, can be assumed fixed as well. The situation is more complicated for low-frequency (about 100 $\rm cm^{-1}$ and lower) solute vibrations. In this case, the shape of the cavity is no longer fixed and there is a part of the orientational polarization which follows solute vibrations. In the GCOSMO approach the dynamical behavior of the cavity and surface charges is reflected in a prescription that is used to calculate derivatives of the matrix $\mathbf{A}$ and the surface charges $\mathbf{q}$. Taking full derivatives of these terms corresponds to the equilibrium solvation. This approach should be taken when studying static properties, such as adiabatic potential energy surfaces. However, an accurate description

of dynamical phenomena, such as solute nuclear vibrations, requires rather complicated frequency-dependent prescription for calculating derivatives of the matrix **A** and surface charges.

In this paper we adopt a simpler approach to this problem. First, we are mostly interested in solvent effects on rather high frequency modes. Thus, the orientational part of surface charges (more than 90% of the total surface charge) and the shape of the cavity can be safely assumed to be fixed. Second, our estimates show that derivatives of the ''electronic'' surface charges make a much smaller contribution to the total second derivatives than the constant term. Therefore, in our expression for second derivatives we simply neglect derivatives of the surface charges (note that this approximation was also adopted in Ref. 26) and matrix **A**. Physically this corresponds to complete nonequilibrium solvation, i.e., the solvent does not respond to solute vibrations at all. Neglecting surface charge derivatives becomes less severe when explicit waters are added to treat strong solute–solvent hydrogen bonding, since the cavity boundary moves farther from the solute in this case. Differentiating Eq. (13) under the above conditions we obtain the following expression

$$\begin{aligned}\frac{\partial^2 E}{\partial y\,\partial x} &= \sum_{\mu\nu} P_{\mu\nu}\frac{\partial^2 H^0_{\mu\nu}}{\partial y\,\partial x} + \frac{1}{2}\sum_{\mu\nu\lambda\sigma} P_{\mu\nu}P_{\lambda\sigma}\frac{\partial^2(\mu\lambda\|\nu\sigma)}{\partial y\,\partial x} \\ &- \sum_{\mu\nu} W_{\mu\nu}\frac{\partial^2 S_{\mu\nu}}{\partial y\,\partial x} + \sum_{\mu\nu}\frac{\partial P_{\mu\nu}}{\partial y}\frac{\partial H^0_{\mu\nu}}{\partial x} \\ &+ \sum_{\mu\nu\lambda\sigma}\frac{\partial P_{\mu\nu}}{\partial y}P_{\lambda\sigma}\frac{\partial(\mu\lambda\|\nu\sigma)}{\partial x} \\ &- \sum_{\mu\nu}\frac{\partial W_{\mu\nu}}{\partial y}\frac{\partial S_{\mu\nu}}{\partial x} + \frac{\partial^2 E_{nn}}{\partial y\,\partial x} + \mathbf{z}^{\dagger}\frac{\partial^2 \mathbf{B}^{\dagger}}{\partial y\,\partial x}\mathbf{q} \\ &+ \sum_{\mu\nu} P_{\mu\nu}\frac{\partial^2 \mathbf{L}_{\mu\nu}{}^{\dagger}}{\partial y\,\partial x}\mathbf{q} + \sum_{\mu\nu}\frac{\partial P_{\mu\nu}}{\partial y}\frac{\partial \mathbf{L}_{\mu\nu}{}^{\dagger}}{\partial x}\mathbf{q}. \quad (14)\end{aligned}$$

The first seven terms in Eq. (14) are the same as for the gas phase second derivatives,[2,35] and the last three terms result from the solute–solvent electrostatic interactions. Positions and values of surface charges **q** should be first determined by GCOSMO geometry optimization. Then, second derivatives can be calculated via Eq. (14) which has a simple interpretation as the Hessian of a molecular species in the field of constant point charges **q**. Due to this reason, Eq. (14) is applicable also for calculating vibrational frequencies with the PCM model under approximations discussed above. Note that this approach leads only to determination of the centers of vibrational bands. In order to obtain their shapes, one needs to perform a Boltzmann averaging over numerous solute and solvent configurations. Currently, such calculations require rather simplified representation of the solute.[12]

C. Computational details

The GCOSMO model presented above was implemented in our locally modified version of the Gaussian 92/DFT computer program.[39] Additional cost for using the GCOSMO model in geometry optimization and frequency calculations in solution is only 10%–20% of that for the free molecule. This allows us to use rather accurate description of the solute wavefunction in this study. First, specific solute–solvent hydrogen bonds were taken into account by explicit consideration of (up to three) nearest water molecules, and geometries of all species were fully optimized using the Berny optimization algorithm. Their coordinates are available upon request. Second, the 6-31+$G(d,p)$ basis set containing diffuse and polarization functions was used in all calculations. Third, we employed a nonlocal hybrid density functional method using the Becke's three-parameter exchange[40] and Lee–Yang–Parr correlation[41] functionals (B3LYP). At this level of theory, the gas-phase experimental vibrational frequencies are reproduced within 5% or better in calculations of molecules in vacuo (see the third columns in Tables I–III, V, and VI).

All parameters of the GCOSMO solvation model (atomic radii, force field parameters for calculation of dispersion and repulsion energies, etc.) were chosen the same as in our previous study.[28] These parameters give an acceptable agreement of the order of 1 kcal/mol with experimental hydration energies for most neutral polar solutes.

TABLE I. Vibrational frequencies and solvent shifts (in cm^{-1}) for acetone.

Mode assignment[a]	Gas phase frequencies		Solvent shifts			
	Expt.[b]	B3LYP	Expt.[b]	GCOSMO	GCOSMO $+H_2O$	Free $+H_2O$
A″ CC t	NO	59	NO	57	51	50
A″ CC t	NO	140	NO	45	37	30
A′ CO sd	385	377	12	14	18	9
A″ CO ob	484	484	10	14	14	2
A′ CO r	530	531	8	9	23	19
A″ CC ss	787	784	8	19	25	10
A′ CC as	872	884	−9	7	9	3
A′ CH_3 r	891	888	17	19	23	15
A′ CH_3 r	1072	1082	−2	12	13	8
A″ CH_3 r	1090	1118	7	8	8	3
A′ CC as	1216	1235	19	27	35	17
A′ CH_3 sd	1355	1385	4	12	14	5
A′ CH_3 sd	1364	1392	3	12	14	10
A′ CH_3 ad	1410	1465	8	6	1	0
A′ CH_3 as	1426	1475	−1	8	7	2
A″ CH_3 ad	1435	1471	−3	−3	−1	−3
A″ CH_3 as	1454	1492	−15	3	1	−1
A′ CO s	1731	1798	−31	−49	−60	−26
A′ CH_3 ss	2920	3035	0	−9	−8	2
A′ CH_3 ss	2937	3042	−10	−9	−7	2
A″ CH_3 as	2972	3096	−9	−6	−5	1
A″ CH_3 as	2972	3103	−2	−5	−4	2
A′ CH_3 as	3004	3156	7	−13	−9	6
A′ CH_3 as	3018	3158	−7	−13	−6	7
Error		52		8	10	6

[a]Abbreviations: *t*=torsion, sd=symmetric deformation, ad=asymmetric deformation, b=bend, ib=in-plane bend, ob=out-of-plane bend, r=rock, s=stretch, ss=symmetric stretch, as=asymmetric stretch, wag=wagging, sc=scissors, tw=twist; A′=in-plane vibration, A″=out-of-plane vibration; NO=not observed.

[b]From Ref. 4, where experimental data for acetone vapour were quoted from Ref. 51.

TABLE II. Vibrational frequencies and solvation shifts (in cm^{-1}) for methylamine.

Mode assignment[a]	Gas phase frequencies		Solvent shifts			
	Expt.[b]	B3LYP	Expt.[c]	GCOSMO	GCOSMO $+H_2O$	Free $+H_2O$
A″ CN t	264	307	NO	95	122	45
A′ NH_2 wag	780	811	175	145	157	100
A″ CH_3 r	NO	973	NO	21	17	12
A′ CN s	1044	1060	−10	−5	−17	−15
A′ CH_3 r	1130	1162	42	37	51	23
A″ NH_2 tw	NO	1342	NO	11	8	−1
A′ CH_3 sd	1430	1459	−2	9	6	4
A′ CH_3 ad	1474	1496	−9	52	14	9
A″ CH_3 ad	1485	1531	−6	0	−1	−11
A′ NH_2 sc	1623	1668	−21	3	−6	−6
A′ CH_3 ss	2820	2963	2	26	42	50
A′ CH_3 as	2962	3071	2	−2	16	29
A″ CH_3 as	2985	3128	−5	−22	−10	7
A′ NH_2 ss	3360	3513	NO	−27	−28	−11
A″ NH_2 as	3424	3604	NO	−41	−44	−19
Error		76		20	14	23

[a]Abbreviations: see footnote a to Table I.
[b]From Ref. 52.
[c]Calculated as a difference between frequencies in aqueous solution measured in Ref. 6 and those from the gas phase (first column).

III. RESULTS

In Fig. 1 we present the GCOSMO optimized structures for acetone$+H_2O$, methylamine$+H_2O$, formic acid$+3H_2O$, acetic acid$+H_2O$, and trans-NMA$+2H_2O$ complexes. Additional calculations showed that selected conformations of methyl groups in acetone, methylamine, and acetic acid in both gas phase and in solution correspond to the lowest energy minimum. Numerous studies[5,8,42–48] suggest that several conformers of NMA can coexist and contribute to the total vibrational spectrum in the gas phase, in solid matrix (where vibrational frequencies for ''free'' NMA were measured[49]), and in aqueous solution. Existing computational methods do not seem to be accurate enough to separate these contributions unambiguously. Therefore we do not intend to explore all conformations and restrict ourselves to qualitative discussion of the solvent effects using one particular example of trans-NMA shown in Fig. 1(e).

All calculated vibrational frequencies for free solutes and their shifts in aqueous solution are listed in Tables I–VI along with available experimental data. Positive values correspond to the blue solvent shift. Note that vibrational modes associated with water molecules are omitted. The first columns in these tables list mode assignments determined by a qualitative analysis of our results. These assignments are generally consistent with potential energy distributions reported earlier; however, in some cases (acetone and NMA) our calculations predict different orders of vibrational modes. The last rows in Tables I–VI contains the averaged unsigned differences between available experimental and our theoretical data. Correlations between observed and calculated frequency shifts are also shown in Figs. 2(a)–2(e).

For acetone, hydration does not induce significant changes in its vibrational spectrum [Table I and Fig. 2(a)]. Calculated frequency shifts do not exceed 60 cm^{-1} and are in

TABLE IV. Solvation shifts (in cm^{-1}) for formic acid calculated in free supermolecule model.

Mode assignment[a]	Experiment[b]	Theory			
		Free +CHELPG	Free $+H_2O$	Free $+2H_2O$	Free $+3H_2O$
A′ CO sd	75	−46	71	82	87
A″ CO(H) t	NO	111	256	272	280
A″ CH(ob)	30	−26	14	25	23
A′ CO(H) s	108	28	87	111	97
A′ OH b	157	−12	92	106	100
A′ CH ib	13	−15	46	51	61
A′ CO s	−67	−77	−43	−66	−54
A′ CH s	4	−15	6	67	35
A′ OH s	NO	−247	−401	−440	−508
Error		69	24	24	26

[a]Abbreviations: see footnote a to Table I.
[b]From Ref. 4.

TABLE III. Vibrational frequencies and solvation shifts (in cm^{-1}) for formic acid.

Mode assignment[a]	Gas phase frequencies		Solvent shifts				
	Expt.[b]	B3LYP	Expt.[b]	GCOSMO	GCOSMO $+H_2O$	GCOSMO $+2H_2O$	GCOSMO $+3H_2O$
A′ CO sd	625	622	75	17	86	94	105
A″ CO(H) t	642	680	NO	31	402	428	435
A″ CH ob	1033	1050	30	−9	−27	−20	−22
A′ CO(H) s	1105	1137	108	41	114	142	136
A′ OH b	1223	1294	157	24	186	188	184
A′ CH ib	1387	1404	13	−3	−15	−1	2
A′ CO s	1776	1820	−67	−45	−73	−87	−77
A′ CH s	2943	3081	4	61	48	54	57
A′ OH s	3570	3732	NO	−49	−671	−744	−801
Error		65		56	26	31	30

[a]Abbreviations: see footnote a to Table I.
[b]From Ref. 4, where experimental data for formic acid vapor were quoted from Ref. 53.

TABLE V. Vibrational frequencies and solvation shifts (in cm^{-1}) for acetic acid.

Mode assignment[a]	Gas phase frequencies		Solvent shifts			
	Expt.[b]	B3LYP	Expt.[b]	GCOSMO	GCOSMO $+H_2O$	Free $+H_2O$
A″ CC t	93	92	NO	49	53	7
A′ CC r	428	423	31	19	27	21
A″ CC ob	535	542	65	17	56	54
A′ CC sd	581	581	45	11	31	33
A″ CO(H) t	639	662	NO	22	334	249
A′ CO(H) s	847	862	47	15	35	28
A′ CH_3 r	987	1002	28	19	29	19
A″ CH_3 r	1044	1068	6	6	6	2
A′ OH b	1181	1206	97	27	115	95
A′ CH_3 sd	1280	1337	84	24	72	59
A′ CH_3 sd	1380	1414	16	13	52	36
A′ CH_3 ad	1434	1476	1	5	8	1
A″ CH_3 ad	1439	1484	−4	5	5	0
A′ CO s	1779	1821	−67	−42	−65	−45
A′ CH_3 ss	2944	3066	1	−16	−17	−2
A″ CH_3 as	2996	3133	−24	−13	−17	−4
A′ CH_3 as	3051	3180	−55	−15	−15	1
A′ OH s	3583	3754	NO	−49	−559	−385
Error		55		25	13	14

[a]Abbreviations: see footnote a to Table I.
[b]From Ref. 4 where experimental data for acetic acid vapor were quoted from Refs. 54 and 55.

TABLE VI. Vibrational frequencies and solvation shifts (in cm^{-1}) for trans-NMA.

Mode assignment[a]	Gas phase frequencies		Solvent shifts			
	Expt.[b]	B3LYP	Expt.[b]	GCOSMO	GCOSMO $+2H_2O$	Free $+2H_2O$
A″ CC t	NO	79*i*	NO	(19)[c]	(28)[c]	(108*i*)[c]
A″ $NC(H_3)$ t	NO	17	NO	129	133	68
A″ NC(O) t	NO	157	NO	26	36	25
A′ CO sd	279	258	18	9	44	32
A′ CO r	429	424	14	9	13	15
A″ NH ob	439	372	NO	204	406	222
A″ CO ob	619	616	NO	36	−1	97
A′ CC s	658	629	−28	3	11	10
A′ NC(O) s	857	877	26	13	24	15
A′ CCH_3 r	980	973	14	17	22	15
A″ CCH_3 r	1037	1055	7	10	12	5
A′ $NC(H_3)$ s	1089	1107	6	5	9	7
A″ NCH_3 r	NO	1156	NO	1	0	0
A′ NCH_3 r	1168	1194	−4	2	1	1
A′ NH ib	1266	1286	46	38	73	41
A′ CCH_3 sd	1370	1398	8	16	22	12
A′ NCH_3 sd	1419	1460	−3	3	5	0
A′ CCH_3 ad	1432	1476	−4	8	10	2
A″ CCH_3 ad	1432	1491	8	2	1	−1
A″ NCH_3 ad	1446	1481	6	16	16	4
A′ NCH_3 ad	1472	1516	−10	3	3	0
A′ NH ib	1511	1555	54,75[d]	36	73	35
A′ CO s	1707	1751	−61,−81[d]	−57	−78	−34
A′ CCH_3 ss	2915	3044	10	−2	1	10
A′ NCH_3 ss	2958	3046	−16	−7	−7	−1
A″ NCH_3 as	2973	3105	0	1	−4	9
A″ CCH_3 as	2973	3107	19	4	4	1
A′ NCH_3 as	3008	3141	12	−3	4	−1
A′ CCH_3 as	3008	3168	1	−12	−8	5
A′ NH s	3498	3647	NO	−60	−174	−95
Error		58		11	10	10

[a]Abbreviations: see footnote a to Table I.
[b]From Ref. 8 where experimental data for isolated NMA were quoted from Ref. 49.
[c]In parentheses, vibrational frequencies are shown instead of shifts.
[d]Splitting of these bands is discussed in Refs. 10 and 47.

agreement with experiment and SQMFF fitting.[4] Solvent shifts are reproduced quite accurately even with the simple GCOSMO solvation model. The average error is only 8 cm^{-1}. Addition of one explicit water molecule (with or without the long-range polarization effects) does not change results substantially.

For methylamine, solvent shifts of vibrational frequencies [Table II and Fig. 2(b)] are generally larger than in the case of acetone. However, similarly to acetone, the simple GCOSMO model reproduces vibrational shifts rather accurately. The average unsigned error is 20 cm^{-1} in this case. Addition of one explicit water molecule making a hydrogen bond with the nitrogen atom slightly improves results of GCOSMO calculations and reduces discrepancy with experiment to 14 cm^{-1}. Inclusion of the long-range polarization contribution within the GCOSMO-supermolecule approach further improves the agreement. This is especially true for the NH_2 wagging mode where free supermolecule approach yields an error of 75 cm^{-1}, while GCOSMO-supermolecule result differs from experiment by only 18 cm^{-1}.

For formic acid, GCOSMO results for vibrational frequency shifts calculated at the simple and supermolecule levels are listed in Table III. The shifts obtained with the free-supermolecule approach are presented in Table IV. All these results are compared with available experimental data in Fig. 2(c). Obviously, the simple GCOSMO model without explicit water molecules (column 5 in Table III) fails to reproduce frequency shifts in formic acid. These large solvent effects are mainly due to hydrogen bonding with water molecule H_6–O_7–H_8 [see Fig. 1(c)]. Explicit treatment of this water molecule in GCOSMO-supermolecule calculations improves the agreement with experiment (the average unsigned error is reduced from 56 to 26 cm^{-1}). Smaller shifts are generally predicted by the free-supermolecule approach with one explicit water (column 4 in Table IV). It is interesting to find out what part of this solvent effect can be attributed solely to the electroctatic potential from the water molecule. To this end, additional calculation of the solute vibrational spectrum was performed by substituting this water molecule by three point charges resulted from the CHELPG fitting procedure. This simple model (see column 3 in Table IV) correctly predicts that the largest shifts are for CO(H) torsion and OH stretching modes; however, their magnitudes are almost twice smaller compared to the calculation with explicit water. Solvent shifts for other modes are more negative than with the full quantum representation of the solvent water. This shows that the electrostatic part of hydrogen bond plays an important but not decisive role in solvent shifts.

Adding more explicit water molecules to GCOSMO- (columns 7 and 8 in Table III) and free-supermolecule (col-

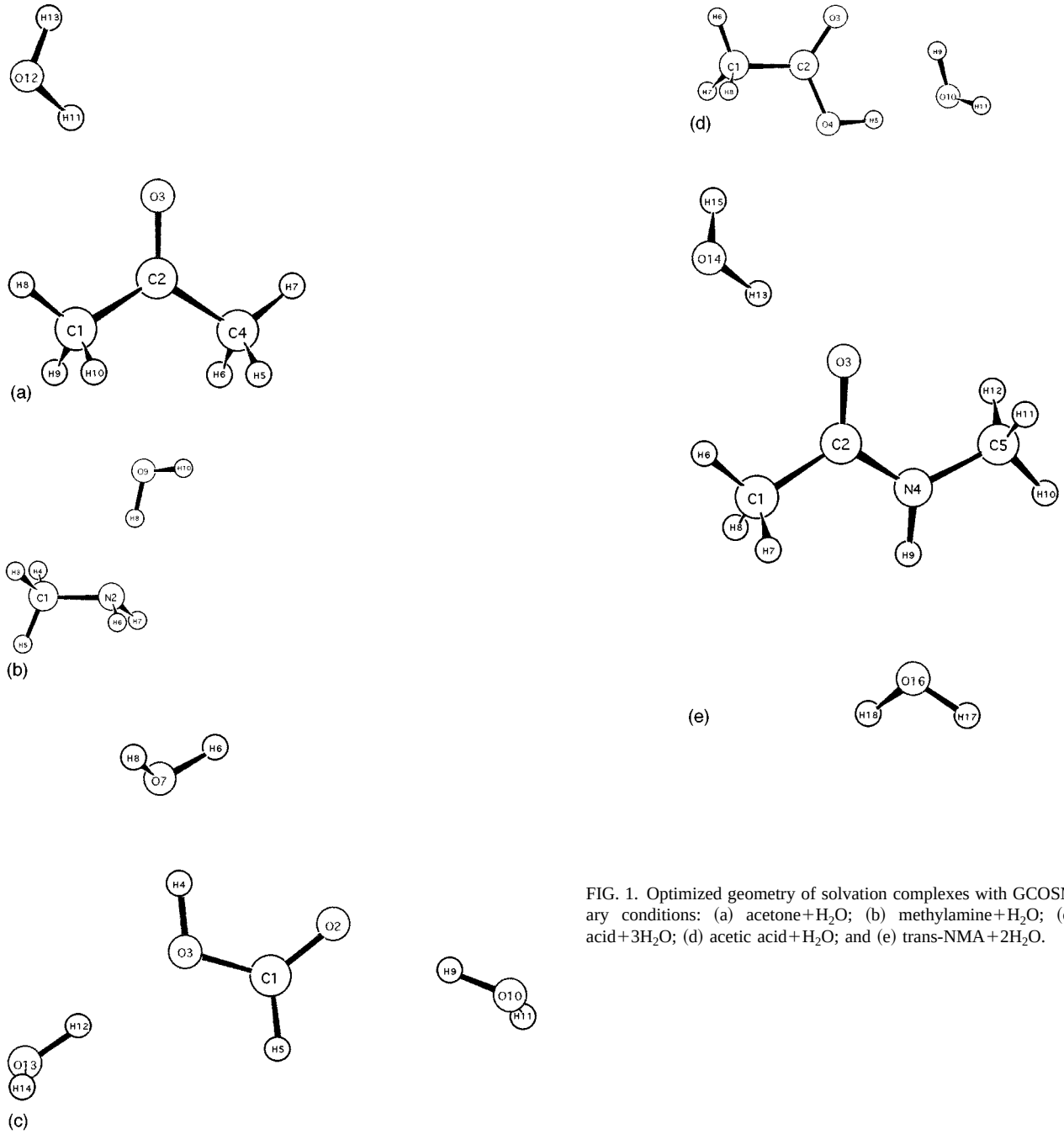

FIG. 1. Optimized geometry of solvation complexes with GCOSMO boundary conditions: (a) acetone+H_2O; (b) methylamine+H_2O; (c) formic acid+$3H_2O$; (d) acetic acid+H_2O; and (e) trans-NMA+$2H_2O$.

umns 5 and 6 in Table IV) calculations do not change results qualitatively: large solvent shifts in CO(H) torsion and OH stretch increase further. The largest discrepancies between GCOSMO- and free-supermolecule results are in these two modes which, unfortunately, were not observed experimentally in solution. In particular, a large frequency shift (more than 400 cm^{-1}) is predicted for CO(H) torsion mode by the GCOSMO-supermolecule method. Using an experimental value (642 cm^{-1}) for this band in the spectrum of a free molecule, we predict that in aqueous solution this band will appear at 1040–1080 cm^{-1}. Free-supermolecule calculations yield values which are smaller by about 150 cm^{-1}. That is consistent with SQMFF fitting which gives the solvent shift of 213 cm^{-1} for the CO(H) torsion.[4] The OH stretch has a negative frequency shift approaching -800 cm^{-1} for GCOSMO with three explicit water molecules. This would result in OH stretching frequency in solution at about 2770 cm^{-1}. Much smaller shifts are predicted by our free supermolecule calculations (about -500 cm^{-1}) and by SQMFF fitting[4] (-554 cm^{-1}). We believe that observed differences between results obtained from GCOSMO- and free-supermolecule calculations are indications of an important long-range polarization effect on vibration spectra. This effect will be discussed in Sec. IV.

For acetic acid, solvent effects on its vibrational spectrum [see Table V and Fig. 2(d)] are qualitatively similar to

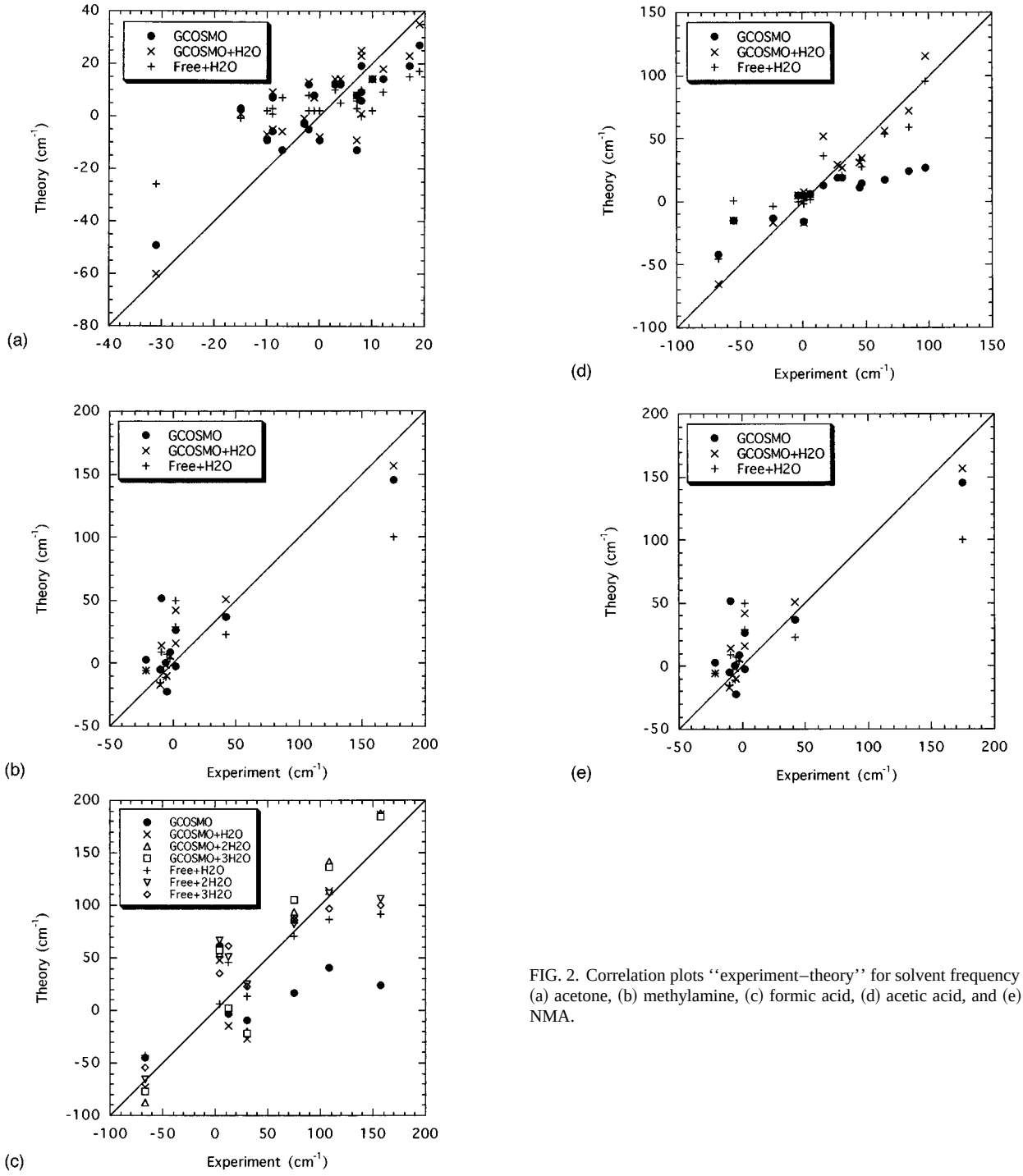

FIG. 2. Correlation plots ''experiment–theory'' for solvent frequency shifts: (a) acetone, (b) methylamine, (c) formic acid, (d) acetic acid, and (e) trans-NMA.

those for formic acid, although somewhat smaller, which indicates weaker hydrogen bonding of acetic acid with water. The simple GCOSMO model underestimates solvent effects. Both GCOSMO- and free-supermolecule results differ from available experimental data by 13–14 cm^{-1}. As in the case of formic acid CO(H) torsion and OH stretching bands have not been observed experimentally. In these cases our GCOSMO-supermolecule results [shifts of 334 cm^{-1} for CO(H) torsion and -559 cm^{-1} for OH stretch] are in better agreement with SQMFF fitting[4] (308 cm^{-1} and -557 cm^{-1}, respectively) than in the case of formic acid. However, based on analogy with formic acid, we can expect that with adding more water molecules the magnitudes of these two shifts would increase. Again, free-supermolecule calculation underestimates values of these shifts by 90–180 cm^{-1}. This provides more evidence for the important role of the long-range polarization effects.

For trans-NMA, we assumed a planar symmetry[48] in all calculations. As remarked above, the prevailing conformers in both gas phase and in solution are not well established.

Variation of vibrational frequencies between different trans-NMA conformers is about 11 cm^{-1} (see Refs. 43 and 46). Therefore, picking only one conformer we cannot expect agreement with experiment better than 11 cm^{-1}. All available experimental frequency shifts in NMA are reproduced within this margin of error with simple GCOSMO solvation model [see Table VI and Fig. 2(e)]. Almost the same level of accuracy is achieved by the GCOSMO- and free-supermolecule models. However, the modes most affected by solvation (NH out-of-plane bend and NH stretch) were not observed experimentally in aqueous solution, thus complete comparison of different models with experiment cannot be made. For these modes, GCOSMO, GCOSMO-supermolecule, and free-supermolecule approaches give rather different results. In particular, inclusion of the long-range polarization effect at the GCOSMO-supermolecule level to the complex of NMA with two water molecules increases the frequency shifts by a factor of 2. This finding is consistent with dielectric polarization effects on CO(H) torsion and OH stretching modes in formic acid and acetic acid.

IV. DISCUSSION

Our calculations suggest that the GCOSMO solvation model predicts rather accurately (average errors 10–20 cm^{-1}) solvent shifts in vibrational frequencies of solutes having moderate strengths of hydrogen bonds with water, such as acetone and methylamine. Also, the simple GCOSMO model gives good results for the majority of modes of trans-NMA. This suggests that for such situations the simple GCOSMO model is quite adequate and one does not need to employ rather expensive supermolecular-continuum calculations. In contrast, for solutes and functional groups having strong hydrogen bonds with water, such as formic acid, acetic acid, and NH group in NMA, the simple GCOSMO approach is not adequate and explicit water molecules should be added in order to take into account specific hydrogen bonds. Comparison of free- and GCOSMO-supermolecule results indicates the importance of *both* hydrogen bond and long-range polarization effects on vibrational modes most affected by the solvent [such as CO(H) torsion and OH stretch in formic acid and acetic acid, NH out-of-plane bend and NH stretch in NMA]. The latter effect cannot be reproduced in the free-supermolecule approach with a small number of explicit water molecules. In this study, the long-range polarization effects are modeled by the GCOSMO continuum approximation. This leads to a significant increase by 80–300 cm^{-1} of vibrational shifts for the modes mentioned above. Unfortunately, experimental results for these modes in aqueous solution are not available. Further experimental studies will help to reveal the relative contributions of local hydrogen bonds and the long-range dielectric polarization effects to vibrational shifts in solutions.

As expected, large solvent shifts in vibrational spectra are accompanied by large changes in the solute structure. In particular, we found that CO, OH, and NH bond distances increase while CO(H) and NC(O) bond distances decrease upon hydration, in agreement with previous findings.[8,33,45,50]

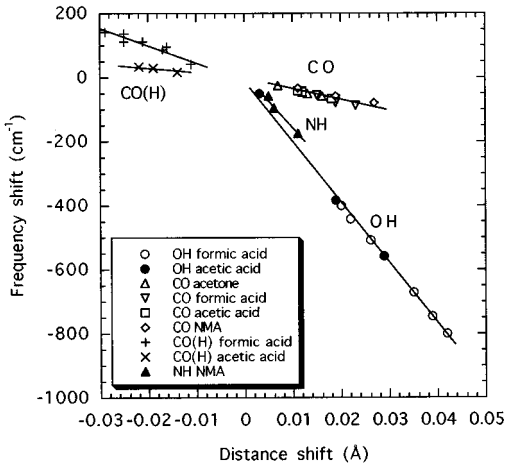

FIG. 3. Correlation plot ''bond distance shift–frequency shift'' for some stretching modes.

An important observation can be made by plotting frequency shifts for stretching modes most affected by solvation [NH,CO,CO(H), and OH stretches] as functions of changes in corresponding bond distances (see Fig. 3). There is an approximate proportionality between the bond elongation (shrinking) and corresponding vibrational frequency shifts. The fitted proportionality coefficients are listed in Table VII. As expected, they are all negative, which corresponds to red frequency shifts for elongated bonds. Moreover, all fitted straight lines intersect at the origin. This corresponds to an intuitive expectation that in the absence of geometry changes the frequency shifts would be very small. Although the OH bond in formic acid and acetic acid is very strong (it has the highest vibrational frequency of 3570–3580 cm^{-1}), this bond is substantially weakened by interaction with the solvent: the bond elongation may be as large as 0.04 Å with corresponding frequency shift of -800 cm^{-1}. This is a manifestation of strong acidic properties of these solutes. It is interesting that correlations ''distance-frequency'' for CO vibrations are almost the same in four studied solutes (acetone, formic acid, acetic acid, and NMA) even though nearest neighbors of the C atom are different in these cases. In contrast, the behavior of the CO(H) stretching mode depends strongly on the immediate environment of the C atoms (H atom in formic acid and CH_3 group in acetic acid). These observations suggest that theoretical determination of solvent vibrational shifts requires quite accurate optimization of the solute geometry. Furthermore, the observed correlation ''geometry–frequency'' allows one to estimate quickly posi-

TABLE VII. Proportionality coefficients α (cm^{-1}/Å) for the linear dependence $\Delta\nu \approx \alpha \cdot \Delta d$ between solvent changes in vibrational frequencies $\Delta\nu$ (cm^{-1}) and in bond distances Δd (Å) for stretching modes shown in Fig. 3.

Mode	α
$(CH_3)CO(H)$	−1452
CO	−3520
(H)CO(H)	−5056
NH	−15 297
OH	−19 324

TABLE VIII. Hydrogen bond distances (Å) for studied solvation complexes.

	Nonsolvated			GCOSMO		
Bond	$+H_2O$	$+2H_2O$	$+3H_2O$	$+H_2O$	$+2H_2O$	$+3H_2O$
Acetone						
$O_3...H_{11}$	1.901			1.850		
Methylamine						
$N_2...H_8$	1.895			1.739		
Formic acid						
$H_4...O_7$	1.767	1.742	1.703	1.658	1.626	1.601
$O_2...H_6$	2.066	2.111	2.189	2.505	3.083	3.210
$O_2...H_9$		1.944	1.971		1.820	1.871
$O_3...H_{12}$			2.052			1.964
Acetic acid						
$H_5...O_{10}$	1.785			1.704		
$O_3...H_9$	1.972			2.332		
NMA						
$O_3...H_{13}$		1.828			1.771	
$H_9...O_{16}$		2.017			1.928	

tions of vibrational bands of important functional groups in aqueous solution by knowing only geometry of the solute and coefficients listed in Table VII.

In addition to bond distances and angles, solvent–solute interaction may alter conformational equilibrium of the solute. For example, the NMA conformer selected for the present study is not stable in the gas phase. This is indicated by an imaginary frequency of $79i$ cm^{-1} of the CC torsion mode in agreement with previous results.[46] This conformer becomes even less stable in the gas phase complex with two water molecules, i.e., CC torsion has even larger imaginary frequency of $108i$ cm^{-1}. However, both simple GCOSMO and GCOSMO-supermolecule calculations yield positive frequencies for all vibrational modes, indicating stable local minimum. This suggests that conformational studies for solvated molecules using supermolecule approach without consideration of the dielectric continuum polarization field may be not accurate.

Dependence of the hydrogen bond distances on the state of solvation (the ''cooperativity'' effect) was observed in calculations for NMA in Refs. 8 and 45 and discussed in detail in Ref. 45. Similar tendencies were observed in our free- and GCOSMO-supermolecule calculations for formic acid (see Table VIII): $H_4\cdots O_7$ bondlength decreases but $O_2\cdots H_6$ distance increases with increasing number of explicit water molecules. Comparison of free- and GCOSMO-supermolecule calculations from Table VIII shows that inclusion of the long-range polarization effects results in large additional bondlength increase (by 0.4–1.0 Å) for the $O_2\cdots H_6$ bond in formic acid (so that this bond is practically broken in the most solvated case) and for similar $O_3\cdots H_9$ bond in acetic acid. The $H_4\cdots O_7$ hydrogen bond distance additionally reduces when the complex is placed in the dielectric cavity. Thus, in these cases the GCOSMO boundary condition has the same effect as the addition of more water molecules in the complex. This shows that, as expected, the GCOSMO-supermolecule model helps in reaching the limit of complete hydration even using small supermolecule clusters. However, this simplistic picture is not true for the $O_2\cdots H_9$ hydrogen bond in formic acid. In this case, addition of water molecule [H_{12}–O_{13}–H_{14} in Fig. 1(c)] increases the $O_2\cdots H_9$ bond distance by 0.03–0.05 Å; however, enclosing the complex in the dielectric cavity reduces this bond distance by 0.10–0.12 Å. This shows a complex nonmonotonic dependence of the cooperativity effect on the state of solvation. Other hydrogen bonds listed in Table VIII decrease by 0.06–0.19 Å when solvated complexes are placed inside the dielectric cavity. A relevant discussion on the relationship between continuum and discrete-continuum models can be found also in Refs. 30–33.

Another effect of the long-range polarization is in changing orientations of water molecules with respect to the solute in GCOSMO-supermolecule calculations. These changes can be seen by comparing structures of solvated complexes of formic acid and trans-NMA in Figs. 1(c) and 1(e) with those in the gas phase (Refs. 4, 7, 8, and 45). The most dramatic example is the water molecule bonded to the NH group in NMA. In the gas phase, this water is oriented perpendicularly to the solute plane (see also Refs. 8, 42, and 45). However, in GCOSMO-optimized structure this molecule is practically in the solute plane. We have no explanation for this, and additional studies are needed to decide whether this is a real physical effect or an artifact of the theoretical model.

V. CONCLUSIONS

We have presented an implementation of the GCOSMO analytical second derivatives and their applications to study solvent shifts in vibrational spectra of acetone, methylamine, formic acid, acetic acid, and trans-N-methylacetamine. This study leads to several important conclusions.

(1) The GCOSMO supermolecule approach provides an efficient tool for both geometry optimization and frequency calculations in polar solvents. Inclusion of the solvent polarization in continuum approximation requires only 10%–20% of additional computational effort as compared with the gas phase calculations. Besides frequency calculations, GCOSMO analytical second derivatives may have important applications in studying free energy surfaces of reactions in solution: optimization of transition state structures, reaction profiles, etc. However, care should be taken in separating effects of equilibrium and nonequilibrium solvation.

(2) Accurate geometry optimization of solvated species is essential for the prediction of vibrational spectra in solution due to correlation between solvent effects on geometry and vibrational frequencies. In particular, solvent shifts in vibrational frequencies of some stretching modes are proportional to changes in corresponding bond distances (see Fig. 3). The knowledge of proportionality coefficients characteristic for each particular functional group (see Table VII) would allow for easy estimate of vibrational shifts using only geometry data.

(3) For molecules with moderate solute–solvent hydrogen bonding, such as acetone and methylamine, the dielectric continuum approach provides rather accurate solvent shifts of vibrational frequencies. For solutes and functional groups exhibiting strong hydrogen bonding with water, such as formic acid, acetic acid, and NH group in NMA, inclusion of at least one water molecule is essential for qualitative prediction of solvent shifts. In these cases, traditional supermolecule approach is not adequate due to neglect of the long-range dielectric polarization field. The GCOSMO-supermolecule calculations allow the reproduction of both specific hydrogen bonding and dielectric polarization effects. More detailed understanding of their relative importance can be obtained after experimental data will become available for most interesting vibrational bands, such as CO(H) torsion and OH stretch in hydrated formic acid and acetic acid and NH out-of-plane bend and NH stretch in hydrated NMA.

ACKNOWLEDGMENTS

This work was supported in part by the University of Utah and by the National Science Foundation through Young Investigator Award to TNT.

[1] K. Miaskiewicz and Z. Kecki, J. Sol. Chem. **19**, 465 (1990).
[2] J. A. Pople, R. Krishnan, H. B. Schlegel, and J. S. Binkley, Int. J. Quant. Chem. Quant. Chem. Symp. **13**, 225 (1979).
[3] G. Fogarasi and P. Pulay, in *Vibrational Spectra and Structure: A Series of Advances*, edited by J. L. Durig (Elsevier, Amsterdam, 1985), Vol. 14, p. 125.
[4] R. W. Williams and A. H. Lowrey, J. Comp. Chem. **12**, 761 (1991).
[5] N. G. Mirkin and S. Krimm, J. Am. Chem. Soc. **113**, 9742 (1991).
[6] A. H. Lowrey and R. W. Williams, J. Mol. Struct. (Theochem) **253**, 35 (1992).
[7] A. H. Lowrey and R. W. Williams, J. Mol. Struct. (Theochem) **253**, 57 (1992).
[8] R. W. Williams, Biopolymers **32**, 829 (1992).
[9] R. W. Williams, V. F. Kalasinsky, and A. H. Lowrey, J. Mol. Struct. (Theochem) **281**, 157 (1993).
[10] X. G. Chen, R. Schweitzer-Stenner, S. A. Asher, N. G. Mirkin, and S. Krimm, J. Phys. Chem. **99**, 3074 (1995).
[11] J. S. Alper, H. Dothe, and D. F. Coker, Chem. Phys. **153**, 51 (1991).
[12] J. S. Alper, H. Dothe, and M. A. Lowe, Chem. Phys. **161**, 199 (1992).
[13] J. Tomasi and M. Persico, Chem. Rev. **94**, 2027 (1994).
[14] M. W. Wong, M. J. Frisch, and K. B. Wiberg, J. Am. Chem. Soc. **113**, 4776 (1991).
[15] M. W. Wong, K. B. Wiberg, and M. J. Frisch, J. Am. Chem. Soc. **114**, 523 (1992).
[16] D. Rinaldi, J. L. Rivail, and N. Rguini, J. Comp. Chem. **13**, 675 (1992).
[17] V. Dillet, D. Rinaldi, J. G. Ángyán, and J. L. Rivail, Chem. Phys. Lett. **202**, 18 (1993).
[18] V. Dillet, D. Rinaldi, and J. L. Rivail, J. Phys. Chem. **98**, 5034 (1994).
[19] S. Miertuš, E. Scrocco, and J. Tomasi, Chem. Phys. **55**, 117 (1981).
[20] R. Cammi and J. Tomasi, J. Chem. Phys. **101**, 3888 (1994).
[21] R. Cammi and J. Tomasi, J. Chem. Phys. **100**, 7495 (1994).
[22] F. J. Olivares del Valle and J. Tomasi, Chem. Phys. **114**, 231 (1987).
[23] F. J. Olivares del Valle, M. Aguilar, S. Tolosa, J. C. Contador, and J. Tomasi, Chem. Phys. **143**, 371 (1990).
[24] M. A. Aguilar, F. J. Olivares del Valle, and J. Tomasi, Chem. Phys. **150**, 151 (1991).
[25] T. N. Truong and E. V. Stefanovich, Chem. Phys. Lett. **240**, 253 (1995).
[26] T. N. Truong and E. V. Stefanovich, J. Chem. Phys. **103**, 3709 (1995).
[27] T. N. Truong and E. V. Stefanovich, J. Phys. Chem. **99**, 14700 (1995).
[28] E. V. Stefanovich and T. N. Truong, Chem. Phys. Lett. **244**, 65 (1995).
[29] A. Klamt and G. Schüürmann, J. Chem. Soc., Perkin Trans. **II**, 799 (1993).
[30] F. R. Tortonda, J. L. Pascual-Ahuir, E. Silla, and I. Tuñon, J. Phys. Chem. **97**, 11 087 (1993).
[31] I. Tuñon, E. Silla, and J. Bertrán, J. Phys. Chem. **97**, 5547 (1993).
[32] I. Tuñon, D. Rinaldi, M. F. Ruiz-López, and J. L. Rivail, J. Phys. Chem. **99**, 3798 (1995).
[33] L. M. Markham and B. S. Hudson, J. Phys. Chem. **100**, 2731 (1996).
[34] B. G. Johnson, P. M. W. Gill, and J. A. Pople, J. Chem. Phys. **98**, 5612 (1993).
[35] B. G. Johnson and M. J. Frisch, J. Chem. Phys. **100**, 7429 (1994).
[36] M. Cossi, B. Mennucci, and R. Cammi, J. Comp. Chem. **17**, 57 (1996).
[37] D. Eisenberg and W. Kauzmann, *The Structure and Properties of Water* (Oxford University Press, New York, 1969).
[38] M. A. Aguilar, F. J. Olivares del Valle, and J. Tomasi, J. Chem. Phys. **98**, 7375 (1993).
[39] M. J. Frisch, G. W. Trucks, H. B. Schlegel, P. M. W. Gill, B. G. Johnson, M. W. Wong, J. B. Foresman, M. A. Robb, M. Head-Gordon, E. S. Replogle, R. Gomperts, J. L. Andres, K. Raghavachari, J. S. Binkley, C. Gonzalez, R. L. Martin, D. J. Fox, D. J. Defrees, J. Baker, J. J. P. Stewart, and J. A. Pople, GAUSSIAN 92/DFT, Revision G.3, Gaussian Inc., Pittsburgh, PA, 1993.
[40] A. D. Becke, J. Chem. Phys. **98**, 1372 (1993).
[41] C. Lee, W. Yang, and R. G. Parr, Phys. Rev. B **37**, 785 (1988).
[42] W. L. Jorgensen and J. L. Gao, J. Am. Chem. Soc. **110**, 4212 (1988).
[43] N. G. Mirkin and S. Krimm, J. Mol. Struct. **242**, 143 (1991).
[44] H.-A. Yu, B. M. Pettitt, and M. Karplus, J. Am. Chem. Soc. **113**, 2425 (1991).
[45] H. Guo and M. Karplus, J. Phys. Chem. **96**, 7273 (1992).
[46] P. L. Polavarapu, Z. Deng, and C. S. Ewig, J. Phys. Chem. **98**, 9919 (1994).
[47] X. G. Chen, R. Schweitzer-Stenner, S. Krimm, N. G. Mirkin, and S. A. Asher, J. Am. Chem. Soc. **116**, 11141 (1994).
[48] N. G. Mirkin and S. Krimm, J. Mol. Struct. (Theochem) **334**, 1 (1995).
[49] S. Ataka, H. Takeuchi, and M. Tasumi, J. Mol. Struct. **113**, 147 (1984).
[50] L. C. Mayne and B. Hudson, J. Phys. Chem. **95**, 2962 (1991).
[51] G. Dellepiane and J. Overend, Spectrochim. Acta **22**, 593 (1966).
[52] Y. Hamada, N. Tanaka, Y. Sugaware, A. Hirakawa, M. Tsuboi, S. Kato, and K. Morokuma, J. Mol. Spectrosc. **96**, 313 (1982).
[53] R. L. Redington, J. Mol. Spectrosc. **65**, 171 (1977).
[54] R. Meyer, T.-K. Ha, H. Frei, and H. H. Günthard, Chem. Phys. **9**, 393 (1975).
[55] C. B. Berney, R. L. Redington, and K. C. Lin, J. Chem. Phys. **53**, 1713 (1970).